

Electrochemical Study of Stabilization Higher Oxidation States of d- and f-Metals in Molten Salts

S.A. Kuznetsov

Institute of Chemistry, Kola Science Centre of Russian Academy of Sciences, 26a Akademgorodok, Apatity, Murmansk region 184209, Russia

*E-mail: kuznet@chemy.kolasc.net.ru

Received: 11 May 2016 / Accepted: 10 June 2016 / Published: 7 July 2016

Conditions of stabilization higher oxidation states of d- and f-metals in molten salts of various anionic and cationic compositions, which determine, respectively, the composition of the first and second coordination spheres of the complexes, have been studied by voltammetry. The stabilization of higher oxidation states is observed when passing from pure chloride to oxochloride melts and from chloride-fluoride to oxofluoride melts. The possibility of stabilization higher oxidation states of chromium in the melts due to the formation of heteronuclear complexes has been demonstrated. It was shown that stabilization of higher oxidation states is accompanied by reaction of disproportionation with formation of fine metal powder in the bulk of the melt and surface coating.

Keywords: molten salts, anionic and cationic compositions, voltammetry, stabilization of higher oxidation states, disproportionation

1. INTRODUCTION

Complex formation is a most widely used method to shift redox equilibrium and, therefore, one of the ways of stabilization various oxidation states in molten salts. To predict *a priori* the stability of d- and f-metals in various oxidation states in molten salt systems is fairly difficult. There are not too much data on stabilization of different oxidation states in molten salts. The largest number of publications related to this problem is devoted to rhenium.

Bailey and Nobile [1] studied electroreduction of K_2ReCl_6 in the LiCl-KCl eutectic at 723 to 823 K, and found that the steady-state voltammogram obtained on a platinum electrode contains only one wave whose half-wave potential is about -0.35 V relative to the platinum reference electrode. This potential is close to the standard electrode potential of the Re(IV)/Re couple, but anodic dissolution of rhenium results in a mixture of Re(III), Re(IV) chloride complexes and Re(III) disproportionate to Re and Re(IV). Disproportionation of Re(III) in the LiCl-KCl melt with formation of metal and Re (IV)

complexes was found also in [2]. Stepanov et al. using the emf method concluded that Re(IV) and Re(V) complexes are present in the NaCl-KCl equimole mixture and determined the apparent standard potentials $E^*_{\text{Re(V)/Re(IV)}}$, $E^*_{\text{Re(IV)/Re}}$, $E^*_{\text{Re(V)/Re}}$ [3]. In study [4] was shown that chlorination of metallic rhenium or ReO_2 by Cl_2 or HCl and dissolution K_2ReCl_6 in the chloride melts of various cationic composition in a wide temperature range led to the formation of Re(IV) complexes which slowly disproportionated forming Re metal and volatile ReCl_5 .

Affoune, Bouteillon and Poignet studied electrochemistry of rhenium in chloride-fluoride melts [5]. Investigating the electrochemical behavior of K_2ReCl_6 in the molten LiF-NaF-KF eutectic (FLiNaK), they found that K_2ReCl_6 cathodically reduces to metal via a reversible two-electron reaction and anodically oxidizes via a reversible one-electron process with the formation of Re(III), which is soluble in the melt. Affoune et al. [5] conclude that, in the FLiNaK melt at temperatures higher than 923 K, the K_2ReCl_6 compound decomposes to thermodynamically stable Re(II) complexes. The same authors in [6] found that solutions of rhenium hexafluoride in molten eutectic mixture at 873 K yielded stable ReF_8^{2-} species, which were reduced via a six-electron irreversible charge transfer step.

Kuznetsov et al. [7] investigated the stability of rhenium complexes and it was found that Re(VI) and Re (VII) oxofluoro or oxo complexes were stabilized in oxofluoride melts depending on the oxygen to rhenium ratio.

Bailey and Nobile [1] state that the formation of rhenium during electrolysis of the LiCl-KCl-K ReO_4 melt at 723 K proceeds by a secondary mechanism. They suggested that lithium cations were first reduced to lithium metal, which interacted with perrhenate ions to yield rhenium metal. Baraboshkin et al. [8] studied electroreduction of KReO_4 in the $\text{Na}_2\text{WO}_4\text{-WO}_3$ melt with various concentrations of the tungsten trioxide. The rhenium cathodic reduction in this melt involved a seven-electron discharge process. In study [9] was shown that solution of KReO_4 in molten LiF-NaF-KF eutectic mixture were stable and their cathodic reduction involved two electrochemical steps, forming Re(VI) and Re (IV) soluble oxocomplexes.

As follows from the above review, there are a many of contradictory data regarding the oxidation states of rhenium.

Stabilization of higher oxidation states of refractory metals after addition of fluoride ions to chloride melts was mentioned in [10, 11].

Nevertheless, no systematic data concerning the influence of melt composition on the stability complexes. This paper is an overview of the author's investigation on stabilization of higher oxidation states of metals in molten salts. The aim of this study is to determine specific features and relationships for stabilization of metal complexes in different oxidation states by varying the anionic and cationic composition of the melt.

2. EXPERIMENTAL

2.1. Chemicals; preparation of salts

Alkali chlorides (LiCl, NaCl, KCl, and CsCl) were purchased from Prolabo (99.5 % min.) for electrochemical measurements. They were dehydrated by continuous and progressive heating just

above the melting point under gaseous HCl atmosphere in quartz ampoules. Excess HCl was removed from the melt by argon. The salts were handled in the glove box and stored in sealed glass ampoules. Fluoride of alkali metals (Aldrich 99.5 % min.) were purified by double melt recrystallization: NaF, KF and CsF were dried in a glassy carbon crucible (SU-2000) at 673-773 K under vacuum, then heated up to a temperature 323 K above its melting point and finally cooled down 323 K below the melting point at a rate of 3-4 K/h. The solidified salts were transferred at 393 K to a dry glove box and impurities were removed mechanically [12, 13].

Pentachlorides of refractory metals were prepared by chlorination of high purity metal powders in a dry chlorine flow. Chlorides of lower oxidation states were synthesized using procedures described in [14] or *in situ* in molten salts due to interaction of refractory metal compounds with own metals [15].

Lanthanide chlorides were prepared by chlorinating the corresponding lanthanide oxides with NH_4Cl . This synthesis includes several steps with a final double distillation ensuring that no residual oxochloride contaminates the lanthanide chloride obtained in this way. However, this method should not be used for synthesis of EuCl_3 and SmCl_3 because of the decomposition tendency of these compounds. Thus, these salts were prepared by chlorinating the oxide (Merck, 99.9) under a stream of high purity argon (water and oxygen less than 2 and 0.5 ppm, respectively) saturated with SOCl_2 or CCl_4 vapors in a quartz reactor at 793 – 813 K for 24 hours [16]. Reduction to dichlorides of europium and samarium were performed by zinc at 773 K during 3 hours under dynamic vacuum [17].

Tetrachloride of uranium was synthesized from U_3O_8 (Merck) by hydrogen reduction to UO_2 and then by chlorination with CCl_4 [18].

All synthesized compounds were identified by chemical analysis and with the aid of X-ray powder diffraction, IR-spectroscopic, and optical crystallography analyses.

2.2. Procedures and electrochemical cell

Salts of alkali metal halides were mixed in required ratio, placed in an ampoule made of glassy carbon (GC) of the SU-2000 type and transferred to a hermetically sealed retort of stainless steel. The latter was evacuated to a residual pressure of 0.7 Pa, first at room temperature and then at higher temperatures (473, 673 and 873 K). After this the retort was filled with high purity argon and the electrolyte was melted.

Linear sweep voltammetry (LSV) and cyclic voltammetry (CV) were employed, using a VoltaLab-40 potentiostat with complementarily packaged software “VoltaMaster 4”, version 6. The potential scan rate was varied between $5 \cdot 10^{-3}$ and 5.0 V s^{-1} . Experiments were carried out in the temperature range 723-1173 K. The voltammetric curves were recorded at different electrodes 0.8-2.0 mm diameter (glassy carbon, several metals) with respect to a glassy carbon plate quasi-reference electrode. The glassy carbon ampoule served as the counter electrode. While the potential of this quasi-reference electrode does not constitute a thermodynamic reference, the use of this electrode was preferred in order to avoid any contact between the melt and oxygen-containing material as used in classical reference electrodes. A Ag/NaCl-KCl-AgCl (2 wt%) reference electrode was used in order to obtain more reliable potential values. At the final stage of each experimental set, this reference

electrode was immersed in the melt for a short time for determination of the potential peaks, the melt being no longer used after these measurements [19, 20].

A X-ray powder diffractometer DRON 2 supplied with computer data processing was used for the identification of the electrolyte phase composition. IR-spectra of quenched melts were recorded with a M-60 Specord, whereas EPR spectra were measured using a ERS-230 unit.

3. RESULTS AND DISCUSSION

3.1. Stabilization of higher oxidation states of *d*-elements by varying the anionic composition

A voltammetric curve of sodium and potassium chloride containing hafnium dichloride is given in Fig. 1, *a*.

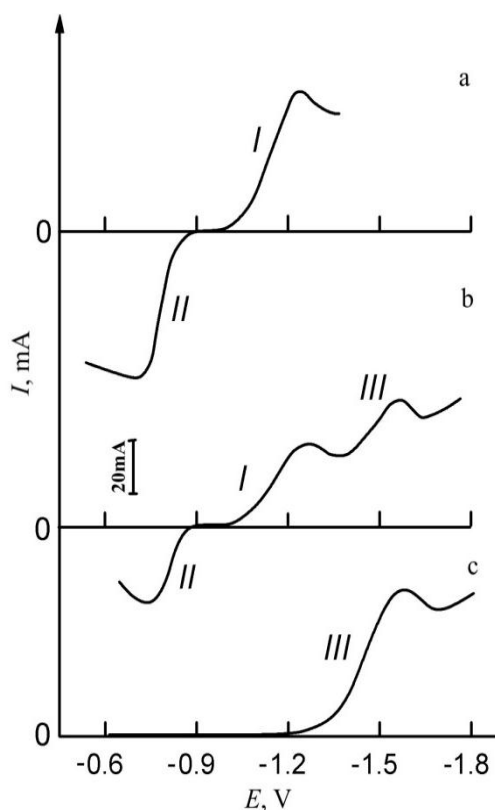


Figure 1. Transformation of voltammetric curves obtained in NaCl-KCl-HfCl₂ melt (*a*) after addition of fluoride ions (*b*, *c*). Sweep rate: 0.7 V s⁻¹. Temperature: 1073 K. Concentration of HfCl₂: 1.98×10⁻⁵ mol cm⁻³. Reference electrode: silver/silver chloride.

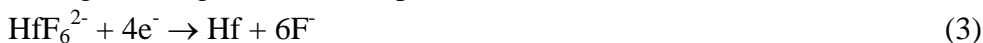
The wave (*I*) on the voltammogram corresponds to irreversible electroreduction [21, 22]:



and wave (*II*) belongs to reversible electrooxidation:



On addition of fluoride anions (concentration ratio $[F]/[Hf] < 3$) peak potential of the processes (1) and (2) shift to the negative region, while additional wave (III) (peak potential -1.56 V) appears in the cathodic region of voltammogram (Fig. 1, b). If $[F]/[Hf] \geq 3$, only one cathodic wave (III) (Fig. 1, c), corresponding to a single irreversible process is observed [23, 24]:



Thus, addition of fluoride anions to the NaCl-KCl-HfCl₂ melt results in stabilization of higher oxidation state of hafnium. This process is accompanied by simultaneous formation of fine hafnium powder, i.e. by disproportionation [23]:



Splitting of cathodic wave at $[F]/[Hf] < 3$ can be caused by formation of hafnium chloride-fluoride complexes as a result of addition of fluoride ions to the melt:



However, at the above given hafnium and fluoride ions ratio the mechanism of chloride-fluoride electroreduction remains to involve two electrons:

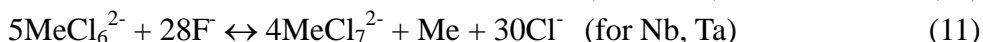
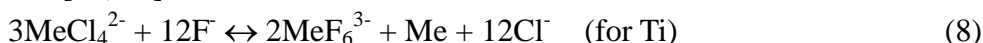


Fluoride ions generated on the electrode interact with chloride-fluoride complexes and displace chloride ions from the first coordination sphere:



Formation of stronger complexes HfF_6^{2-} near the electrode surface causes, as in the case of potentiometric titration, the shift of potential that results in appearance of additional wave corresponding to process (3) on the voltammetric curve.

By sodium fluoride titration of chloride melts equivalence points of chlorine ligands substitution by fluoride ions in the first coordination sphere of d-metal complexes have been established [25, 26]:



Reactions equivalence points were determined as a moment of complete transition from one electrode reaction mechanism to another. When fluoride ions are added to NaCl-KCl melt containing chromium trichloride, the number of electroreduction stages remains the same, because in the melt fluoride complexes of the same oxidation state are formed [27-31]. It should be noted that equivalent points of reactions (8)-(11) are always reached at slightly lower $[F]/[\text{Me}]$ ratio. This shows that, along with fluoride complexes, the chloride-fluoride complexes are present in the melt.

Reaction of stabilization of higher oxidation states of d-metals can be not only homogeneous, but also heterogeneous. The data on niobium electroreduction in LiCl-KCl-NbCl₅ melt show that discharge at temperature low than 903 K is a three-stage process [32]. The cathodic voltammograms obtained on platinum at 733 K are presented in Fig. 2. The potentiostatic electrolysis at potentials of the second wave results in formation of various cluster compounds NbCl_x on the cathode. Moreover, electrolysis at different potentials permits preparing compounds with niobium content from 45 to 54 wt%, i.e. $\text{NbCl}_{2.33}$ and compounds $\text{NbCl}_{2.67}$ - $\text{NbCl}_{3.13}$ composition [32, 33].

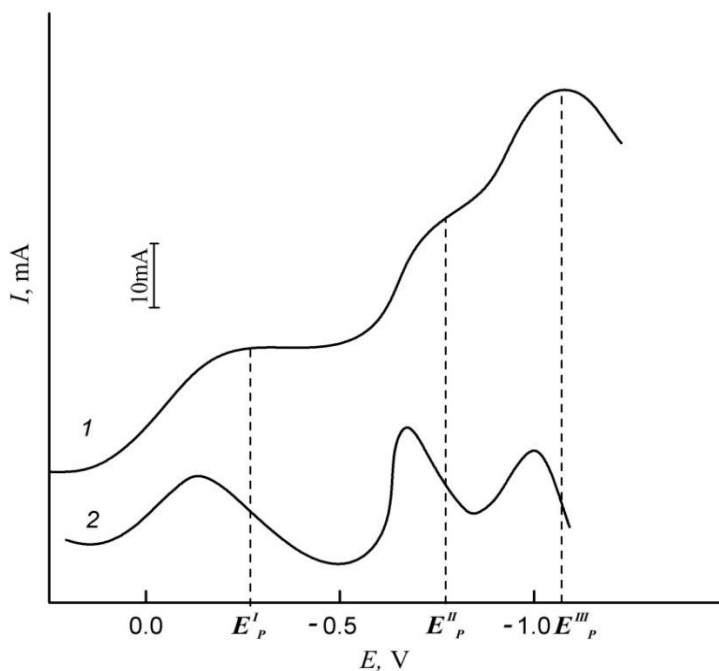
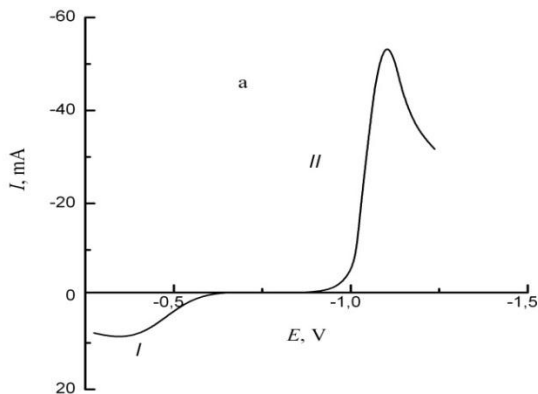


Figure 2. Voltammograms of LiCl-KCl-NbCl₅ melt. 1-integral curve. 2-differential curve. Sweep rate: 0.7 V s⁻¹. Temperature: 733 K. Concentration of NbCl₅: 3.12×10⁻⁵ mol cm⁻³. Reference electrode: silver/silver chloride.

Addition of ions causes dissolution of cluster compounds and formation of NbF₆²⁻ complexes and metallic niobium in the melt. The voltammetric curve of the melt after introduction of fluoride ions already contains two waves (Fig. 3, a): wave (I) in the anodic region, which corresponds to the oxidation of Nb(IV) complexes to Nb(V) ones, and wave (II) in the cathodic region, corresponding to reduction of Nb(IV) to Nb-metal [34, 35].



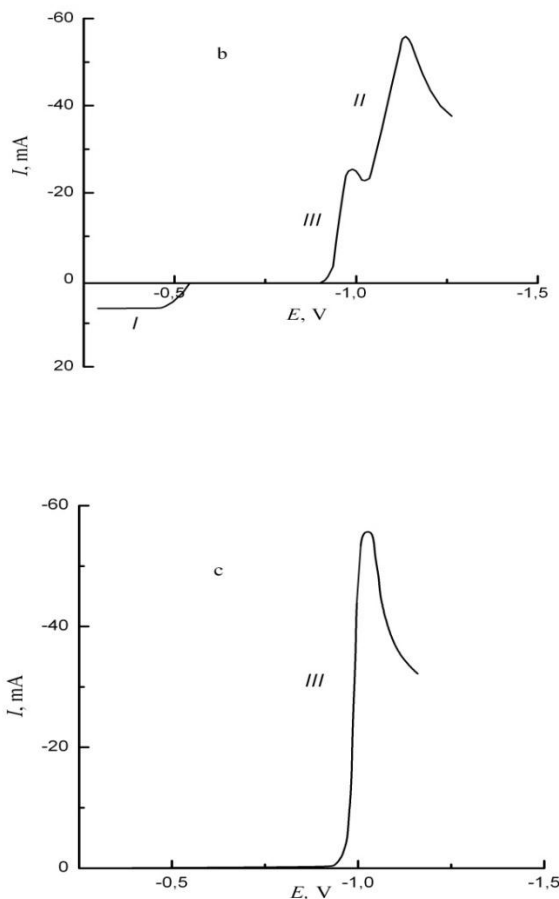


Figure 3. Transformation of voltammetric curves obtained in NaCl-KCl melt containing Nb(IV) complexes. Sweep rate: 0.7 V s^{-1} . Temperature: 1023 K. Concentration of Nb(IV): $8.61 \times 10^{-5} \text{ mol cm}^{-3}$. Molar ratio [O]/[Nb]: a) 0; b) 0.4; c) 0.8. Reference electrode: silver/silver chloride.

Niobium oxidation state can be elevated to +5 by introduction of oxide ions in the form of niobium or sodium and calcium oxides to the chloride fluoride melt. In this case, the following transformations of voltammogram are observed: intensity of the waves corresponding to electroreduction-electrooxidation of the niobium fluoride complexes decreases and a new wave (III) in the cathodic region appears (Fig. 3, b).

Finally, at a certain ratio of niobium and oxide ions described by reaction [36, 37]:



Only a single discharge wave (III) of NbOF_6^{3-} remains on the voltammetric curve (Fig. 3, c) [36, 38].

The reaction (12) was used for production of niobium coatings on oxide materials [24].

Stabilization of higher oxidation states occurs also during formation of complexes with oxygen ions in the pure chloride melts. On addition of Na_2O , BaO or CaO to the melts containing lowest titanium, zirconium, or hafnium chlorides (at the certain MeO to MeCl_2 ratio) only the waves

corresponding to NaCl-KCl melt are registered on the voltammograms. Barium and calcium cations have more negative discharge potentials than alkali metal cations. Analysis of the upper parts of solidified electrolytes shows only the trace amounts of Ti, Zr, or Hf. According to XRD analysis the bottom part of electrolytes consists mainly of titanium, zirconium or hafnium oxides, while walls of the cell are plated by metallic coating. In the case of hafnium, these obtained facts can be explained by the reaction [26]:



Changes of the oxidation states of d-elements (refractory metals) in NaCl-KCl molten salt from pure chloride to oxochloride, chloride-fluoride and oxofluoride complexes are given in Table.

Table. Oxidation states of d-metals in the NaCl-KCl melt

3d (*)	Composition of complexes				4d (*)	Composition of complexes				5d (*)	Composition of complexes			
	Cl	O-Cl	Cl-F	O-F		Cl	O-Cl	Cl-F	O-F		Cl	O-Cl	Cl-F	O-F
Ti	II-IV	III, IV	III, IV	IV	Zr	II, IV	IV	IV	IV	Hf	II, IV	IV	IV	IV
Cr	II,III	III,V, VI	II, III	VI	Nb	IV-V	V	IV,V	V	Ta	IV-V	V	V	V
										Re	III, IV	V-VII	III, IV	VI, VII
										Ir	III, IV	V, VI	IV	VI

*) - elements; Cl-chloride; O-Cl-oxochloride; Cl-F-chloride-fluoride; O-F- oxofluoride

The stabilization of higher oxidation states is often observed when passing from pure chloride to oxochloride melts and from chloride-fluoride to oxofluoride melts. These data show that anionic ligands as F⁻ and O²⁻ are preferable for stabilizing highest oxidation states. In fact, electron deficit at the ion in highest oxidation state causes its instability. That is why ligand has to compensate this electron deficit by transferring its electron pair on the free orbitals of central ion. Moreover, this ligand must be electronegative enough to exclude the irreversible electron transfer [39, 40].

Fluoride complexes of rhenium ReF₆²⁻ in chloride-fluoride NaCl-NaF melt discharge to the metal via a two-stage process (Fig. 4 a) [7, 40]. The addition of oxygen anions in the NaCl-NaF eutectic melt containing rhenium leads to a decrease in the height of waves corresponding to the discharge of rhenium from the fluoride complexes, while at more negative potentials, two extra waves appear (Fig. 4 b). When the mole ratio of oxygen anions and rhenium is close to the stoichiometry of the reaction:



waves (I) and (II) cannot be observed, and the voltammograms display only waves (III) and (IV) with increased heights (Fig. 4 c) [40].

Reaction (14) is confirmed by the rhenium dispersion in the bulk of the melt and by the IR-spectra of the quenched melt [41].

Further addition of oxygen anions results in the formation of dioxofluoride complexes of rhenium:



These can be identified due to the appearance of three groups of doublets in the IR-spectra [42]. The formation of dioxofluoride complexes causes changes in the voltammograms, namely, wave (III) disappears while wave (IV) is enhanced (Fig. 4 d).

Upon further increase in the oxygen anion content in the melt the voltammetric curve takes on the shape that is characteristic of the background curve (Fig. 4e) [7, 40].

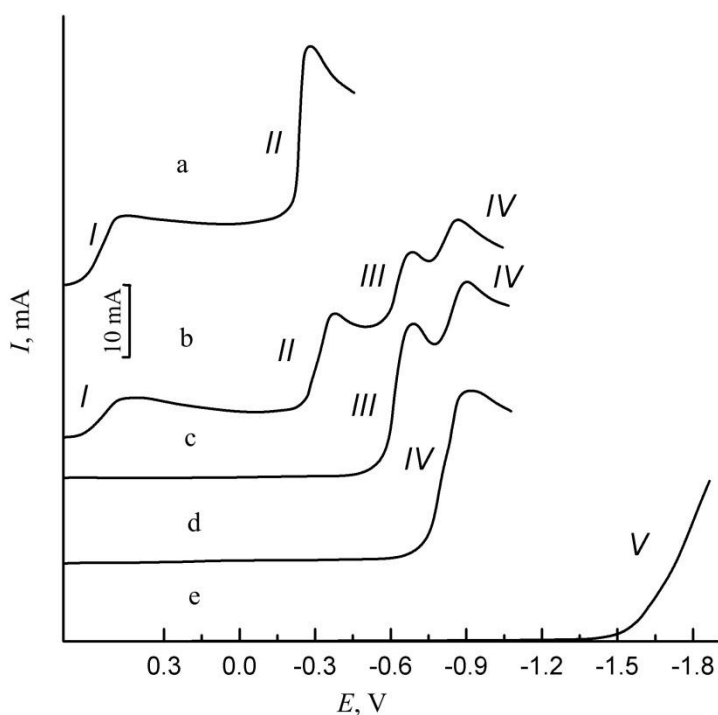
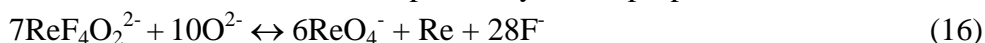


Figure 4. Transformation of voltammograms obtained in NaCl-NaF eutectic melt after introduction of oxygen ions into the melt. Sweep rate: 0.25 V s^{-1} . Temperature: 1023 K. Concentration of rhenium: $5.63 \times 10^{-5} \text{ mol cm}^{-3}$. Reference electrode: silver/silver chloride. Molar ratio [O]/[Re]: a 0; b 0.32; c 0.67; d 1.33; e 2.3.

Infrared spectra of quenched samples display only absorption bands that are characteristic of the compound NaReO_4 [42]. Thus, obtained results demonstrate that perrhenates are formed in the melt, and that their formation is accompanied by the disproportionation reaction [40]:



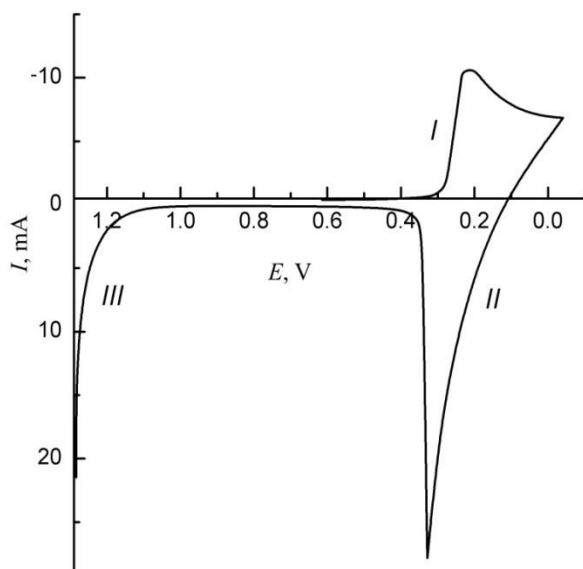
3.2. Stabilization of higher oxidation states of *d*-elements by varying the cationic composition

Figure 5. Cyclic voltammogram of NaCl-ReCl₃. Sweep rate: 0.5 V s⁻¹. Temperature: 1123 K. Concentration of ReCl₃: 2.34×10⁻⁵ mol cm⁻³. Reference electrode: silver/silver chloride.

All data given above refer to the stabilization of higher oxidation states due the changes of the first coordination sphere complexes, while in some case oxidation state of *d*-metals may be increased by variation of second coordination sphere composition.

During electrochemical study of rhenium in NaCl melt [40] (metal concentration was defined by direct chlorination of rhenium in the melt) cyclic voltammogram demonstrates a single reduction peak (*I*) of rhenium complex, corresponding peak of metal electrooxidation (*II*), and a wave (*III*) of chlorine evolution (Fig. 5). Calculation of the transferred number electrons shows that three-electron transfer during electroreduction to metal. So, only Re(III) complexes are present in NaCl melt.

As for chlorination of rhenium in KCl and CsCl melts, investigations show that Re (IV) complexes are formed. On mixing of NaCl melt containing rhenium with KCl and CsCl melts, the displacement of sodium cations from the second coordination sphere by potassium and cesium ones and formation of Re (IV) complexes are observed. Formation of Re (IV) complexes was registered by appearance of Re (III) – e⁻ → Re(IV) electrooxidation wave (*IV*) on the cyclic voltammogram (Fig. 6) [7, 40]. In the NaCl-KCl system Re(IV) complexes are formed at 60 mol% KCl, while for NaCl-CsCl melt this occurs at CsCl concentration of 75 mol%. Higher concentration of CsCl is required due to lower ionic potential as compared to potassium.

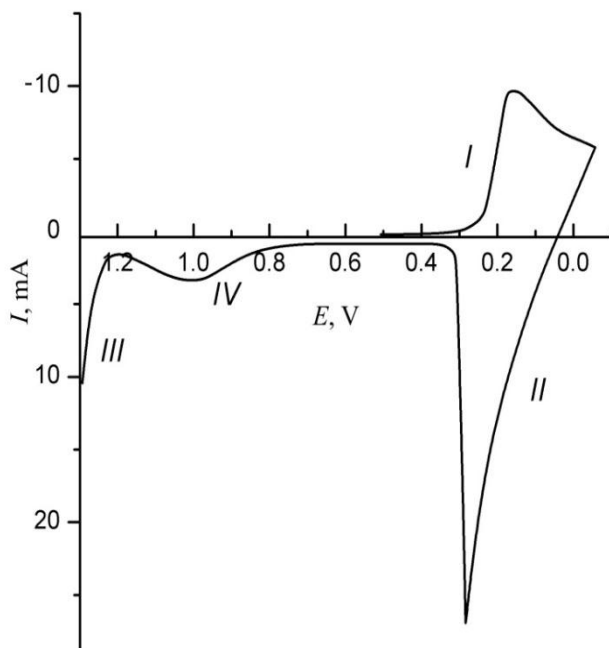


Figure 6. Cyclic voltammogram of NaCl (40 mol%)-KCl (60 mol%) melt containing rhenium. Sweep rate: 0.5 V s^{-1} . Temperature: 1023 K. Concentration of ReCl_4 : $2.64 \times 10^{-5} \text{ mol cm}^{-3}$. Reference electrode: silver/silver chloride.

As shown in studies [24, 33], on addition of CsCl in amounts greater than or equal to 70 mol% to the NaCl-KCl-HfCl₂ melt leads to disproportionation:



Substitution of sodium and potassium by cesium cations (ionic potential of cesium is lower in comparison with sodium and potassium and substitution is possible if concentration CsCl \geq 70 mol%) is accompanied by stabilization of highest oxidation state of hafnium and simultaneous formation of metal powder in the bulk of the melt and metallic film on the surface of crucible.

The results obtained can be explained by competition of the bond formation between chlorine and transition metal (first coordination sphere) and between chlorine and alkali metal of the second coordination sphere. The higher ionic character of this bond, the higher is effective charge of chlorine and, respectively, the more covalent the d-element-chlorine bond becomes [43]. Increase in bond covalence stabilizes the complex. Therefore, cesium is preferable, among alkali metals, for stabilizing higher oxidation states of metals in the melts.

On the basis of Lux concept [44] we may conclude that increase of the melt basicity results in stabilization of higher oxidation states of d-metals. In some cases, stabilization can be achieved by increasing the melt basicity through changing not only anionic, but also cationic composition.

It should be noted that in aqueous solutions higher oxidation states of all transition metals are also stabilized in alkali solutions and destabilized in acidic solutions [39].

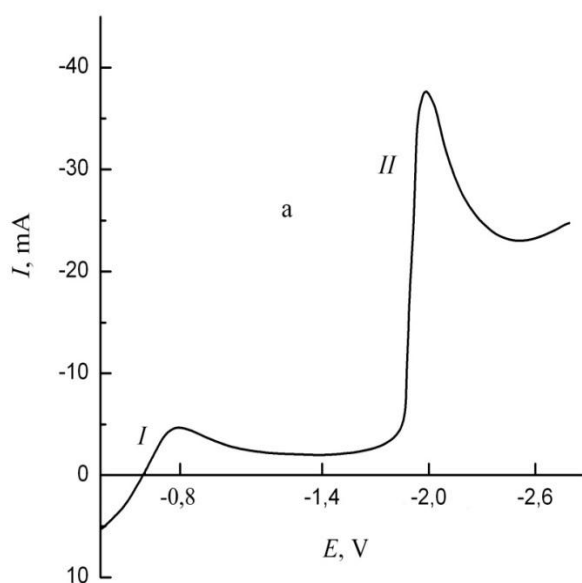
3.3. Stabilization of higher oxidation states of *d*-elements due to the formation of heteronuclear complexes

Another possibility of increasing metal oxidation states in molten salts is formation of heteronuclear complexes.

The voltammogram of the NaCl-KCl melt containing Cr(II) and Cr(III) complexes has two peaks (Fig. 7a). Anodic-cathodic peak (*I*) at potential of -0.7 V corresponds to the $\text{Cr(II)} + e^- \leftrightarrow \text{Cr(III)}$ electroreduction-electrooxidation process. Cathodic peak (*II*) at the potential -1.9 V characterizes the following reduction process: $\text{Cr(II)} + 2e^- \rightarrow \text{Cr}$ [29]. The addition of AlCl_3 in the melt leads to a decrease in peak heights (*I* and *II*), and a new sharp peak (*III*) appears at potential of -1.6 V (Fig. 7 b). In the presence of AlCl_3 peak (*III*) appears due to the formation of electrochemically active species (EAS) other than Cr(II) and Cr(III) complexes. New EAS are heteronuclear complexes of chromium and aluminium [45].

The energy and time of reorganization of complexes are known to markedly decrease in the presence of bridge species [33]. Therefore, probably, the discharge of heteronuclear complexes of chromium and aluminium, in which the metal-metal bond breaks across the bridges, occurs at more positive potentials than the potential of Cr deposition from Cr(II) complexes. Raman and IR-spectra of NaCl-KCl quenched melts containing chromium and aluminium compounds (in contrast to these spectra for individual compounds) exhibit new lines. Apparently, these lines characterize the heteronuclear complexes. As shown by electron paramagnetic resonance (EPR) analysis of quenched melts, the addition of AlCl_3 in the melt (in which the ratio between Cr(II) and Cr(III) is 30:1) leads to an increase in the Cr(III) concentration by 10-12 times (Fig. 8).

Moreover, quenched melt samples change their color from green to pink, which is characteristic of the Cr(II) and Cr(III) complexes, respectively.



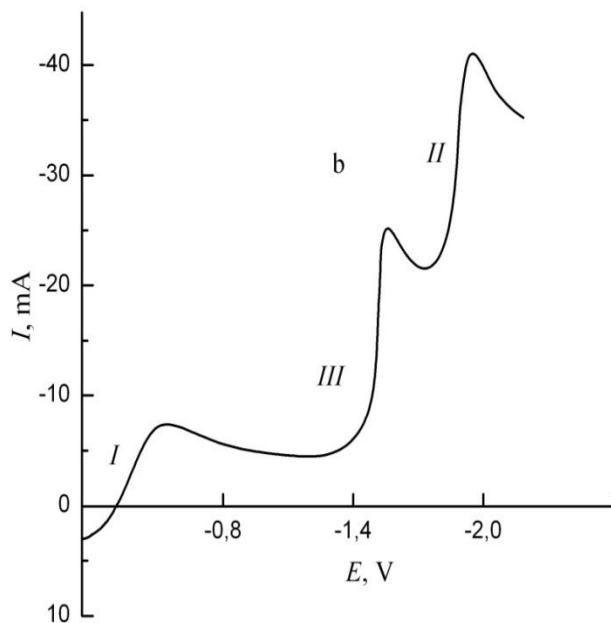


Figure 7. Transformation of voltammogram for NaCl-KCl-CrCl₂-CrCl₃ melt: (a) without AlCl₃; (b) with AlCl₃. Concentration of chromium: 6.23×10^{-5} mol cm⁻³. Molar ratio [Al]/[Cr] = 1:2. Sweep rate: 0.5 V s⁻¹. Temperature: 1023 K. Reference electrode: silver/silver chloride.

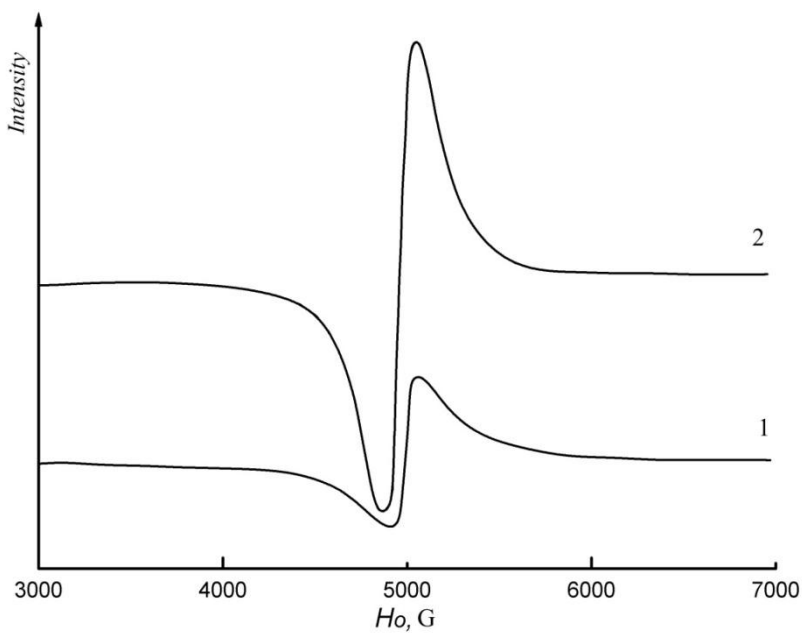


Figure 8. Variation in intensity of EPR spectrum for Cr(III) complexes: (1) NaCl-KCl-CrCl₂-CrCl₃ melt; (2) after the addition of AlCl₃ in the melt (1). Concentration of chromium: 9.21×10^{-5} mol cm⁻³. Molar ratio [Al]/[Cr] = 1:1.5.

Note that the formation of neutral heteronuclear complexes of chromium and aluminium, $\text{Cr}(\text{Al}_2\text{Cl}_7)_2$, in the AlCl_3 melt at a temperature 500 K was established in investigation [46]. In our case, the heteronuclear complex formation is accompanied by stabilization of Cr(III), presumably by the following reaction:



Stabilization of Cr(III) occurs simultaneously by the formation of chromium [45].

3.4. Stabilization of higher oxidation states of f-elements

The abovementioned conclusion that the melt basicity leads to stabilization of higher oxidation states is also valid for f-metals. Some lanthanides, e.g., Nd, Sm, Eu, and Yb, exist in molten chlorides in the oxidation state +2. Once oxygen anions have appeared in the system, which is, among other factors, due to corrosion of oxide materials, the oxochloride or oxide of a lanthanide in oxidation state +3 forms. This process is accompanied by dispersion of a rare earth metal over the bulk of the melt [47]. Among the lanthanides, of prime interest is cerium for which the oxidation state +4 is most stable as compared with the other elements in the series. The synthesis of Cs_2CeCl_6 has been described [48]. This compound starts decomposing to form Ce(III) and chlorine at temperatures above 603 K in an inert atmosphere. Thus, in molten chlorides, lanthanides in the oxidation state +4 are unstable and are potent oxidants for chloride anions, according to the reaction:



At the same time, Ce(IV) can exist in molten chlorides at chlorine pressures considerably exceeding atmospheric pressure. In particular, on the basis of specific electroconductivity measurements, it has been demonstrated that, in the CsCl-CeCl_3 melt containing 13 mol % CeCl_3 at a chlorine pressure of 9 atm, Ce(III) and Ce(IV) complexes coexist in nearly equal amounts [49].

In molten fluorides, it is easy to create the $\text{CeF}_3/\text{CeF}_4$ redox couple, which controls the corrosion of the material of a liquid-salt reactor in the LiF-BeF_2 melt [50].

Transformation of the voltammetric curves caused by the introduction of oxide ion O^{2-} (Li_2O) into LiCl-KCl-UCl_4 melt is shown in Fig. 9. After the addition of Li_2O in the molten system containing UCl_4 , waves R_1 and R_2 corresponding to the discharge of the uranium chloride complexes decreased (Fig. 9 a), and two new waves, R_3 and R_4 , appeared in the voltammetric curve (Fig. 9 b). At the molar ratio $\text{O}^{2-}/\text{U(IV)} = 1.3 - 1.5$, the voltammetric curves showed only waves R_3 and R_4 , (Fig. 9 c), and the melt was yellow, which is evidence of formation of U(VI) complexes [18].

The following chemical reaction can be suggested to occur in the melt:



Indeed, the introduction of UO_2Cl_2 into the melt led to an increase in the heights of waves R_3 and R_4 ; and these waves are related to the discharge of the uranyl-chloride complexes [51]:



Thus, in the oxochloride melt, uranium is stabilized in the highest oxidation state (+6) in the form of uranyl-chloride complexes.

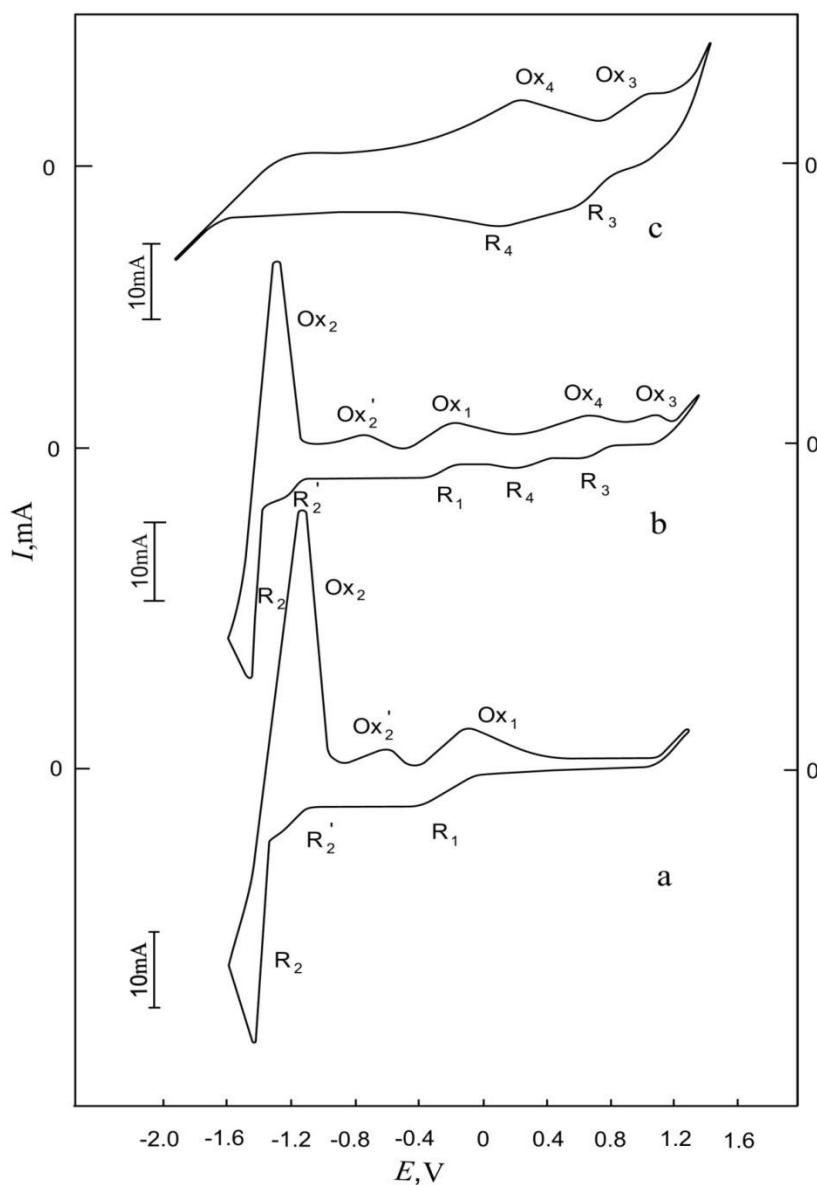


Figure 9. Cyclic voltammograms obtained on a tungsten electrode in the LiCl-KCl-UCl₄ melt. The O²⁻/U(IV) ratio was (a) 0, (b) 0.23, and (c) 1.4. Initial UCl₄ concentration 4.61×10^{-5} mol cm⁻³. Sweep rate, 0.5 V s⁻¹. Temperature: 723 K. Reference electrode: silver/silver chloride.

4. CONCLUSIONS

Electrochemical studies which accompanied by XRD and IR, EPR spectroscopy have shown that the increase in the melt basicity leads to stabilization of higher oxidation states of both d- and f-elements. The increase in the oxidation state of metals caused by a change in the composition of a molten reaction medium can be used for their separation and for carrying out the disproportionation reactions in molten salts to produce ultrafine metal powders and coatings.

References

1. R.A. Bailey, and A.A. Nobile, *Electrochim. Acta*, 17 (1972) 1139-1149
2. A.D. Stepanov, S.N. Shkol'nikov, A.M. Ezrokhina, *Izv. Vyssh. Zaved., Tsvetn. Metallurg.*, 5 (1985) 65-67.
3. R.A. Bailey, and J.A. McIntyre, *Inorg. Chem.*, 5 (1966) 1940-1942.
4. D. Danilov, V.A. Volkovich, and B.D. Vasin, *Z. Naturforsch.*, 63a (2008) 371-376.
5. A. Affoune, J. Bouteillon, and J.C. Poignet, *Proceedings of the 7 International Symposium on Molten Salts*, 90(17) (1990) 471-480.
6. A. Affoune, J. Bouteillon, and J.C. Poignet, *J. Appl. Electrochem.*, 32 (2002) 521-526.
7. S.A. Kuznetsov, A.B. Smirnov, A.N. Shchetkovsky, and A.L. Etenko, *Refractory Metals in Molten Salts*, Kluwer Academic Publisher, Dordrecht 3/53 (1998) 219-226.
8. A.N. Baraboshkin, V.P. Bychin, and O.N. Vinogradov-Zhabrov, *Soviet Electrochemistry*, 14 (1978) 155-159.
9. A. Affoune, J. Bouteillon, and J.C. Poignet, *J. Appl. Electrochem.*, 25 (1995) 886-889.
10. A.N. Baraboshkin, *Electrocrystallization of Metals from molten Salts*, Moscow, Nauka, 1976.
11. D. Inman, S.H. White, *J. Appl. Electrochem.*, 8 (1978) 375-390.
12. S.A. Kuznetsov, M. Gaune-Escard, *J. Nucl. Mater.*, 414 (2011) 126-131.
13. A.V. Popova, S.A. Kuznetsov, *J. Electrochem. Soc.*, 163 (2016) H53-58.
14. G. Brauer, W.P. Fehlhhammer, and O. Glemser, *Handbuch der Preparativen Anorganischen Chemie*, Ferdinand Enke Verlag, Stuttgart, 1981.
15. A.V. Popova, V.G. Kremenetsky, S.A. Kuznetsov, *J. Electrochem. Soc.*, 161 (2014) H447-452.
16. L. Rycerz, *Thermochemistry of lanthanide halides and compounds formed in lanthanide halide-alkali metal halide systems*, Wroclaw University of Technology, 2004.
17. S.A. Kuznetsov, M. Gaune-Escard, *Electrochim. Acta.*, 46 (2001) 1101-1111.
18. S.A. Kuznetsov, H. Hayashi, K. Minato, M. Gaune-Escard, *J. Electrochem. Soc.*, 152 (2005) C203-205.
19. S.A. Kuznetsov, M. Gaune-Escard, *J. Electroanal. Chem.*, 595 (2006) 11-22.
20. A.V. Popova V.G. Kremenetsky, S.A. Kuznetsov, *ECS Trans.*, 64(4) (2014) 171-182.
21. S.A. Kuznetsov, S.V. Kuznetsova, P.T. Stangrit, *Russ. J. Electrochem.*, 26 (1990) 55-60.
22. S.A. Kuznetsov, S.V. Kuznetsova, P.T. Stangrit, *Russ. J. Electrochem.*, 26 (1990) 98-101.
23. S.A. Kuznetsov, S.V. Kuznetsova, P.T. Stangrit, *Russ. J. Electrochem.*, 28 (1992) 236-239.
24. S.A. Kuznetsov, *Pure Appl. Chem.*, 81 (2009) 1423-1439.
25. S.A. Kuznetsov, E.G. Polyakov, P.T. Stangrit, *Melts*, 2 (1987) 81-85.
26. S.A. Kuznetsov, *Refractory Metals in Molten Salts*, Kluwer Academic Publisher, Dordrecht 3/53 (1998) 189-196.
27. Yu.V. Stulov, S.A. Kuznetsov, *ECS Trans.*, 33(7) (2010) 329-335.
28. Y.V. Stulov, V.G. Kremenetsky, O.V. Kremenetskaya, A.D. Fofanov, S.A. Kuznetsov, *Russ. J. Electrochem.*, 47 (2011) 948-958.
29. Y.V. Stulov, V.G. Kremenetsky, S.A. Kuznetsov, *ECS Trans.*, 50(11) (2012) 135-152.
30. Y.V. Stulov, V.G. Kremenetsky, S.A. Kuznetsov, *Int. J. Electrochem. Sci.*, 8 (2013) 7327-7344.
31. Y.V. Stulov, V.G. Kremenetsky, S.A. Kuznetsov, *Russ. J. Electrochem.*, 50 (2014) 907-916.
32. S.A. Kuznetsov, A.G. Morachevskii, P.T. Stangrit, *Soviet Electrochem.*, 18 (1982) 1522-1526.
33. S.A. Kuznetsov, *Molten Salts: From Fundamentals to Applications*, Kluwer Academic Publisher, Dordrecht II/52 (2002) 283-303
34. A.V. Popova, S.A. Kuznetsov, *Russ. J. Electrochem.*, 44 (2008) 921-925.
35. A.R. Dubrovskiy, M.A. Okunev, O.V. Makarova, E.A. Mahaev, S.A. Kuznetsov, *Russ. J. Appl. Chem.*, 89 (2016) 80-86.
36. S.A. Kuznetsov, E.A. Marenkova, V.T. Kalinnikov, *Doklady Chemistry*, 463 (2015) 169-173.
37. S.A. Kuznetsov, V.T. Kalinnikov, *Doklady Chemistry*, 460 (2015) 37-40.

38. V.V. Grinevitch, V.A. Reznichenko, M.S. Model, S.A. Kuznetsov, E.G. Polyakov, P.T. Stangrit, *J. Appl. Electrochem.*, 29 (1999) 693-702.
39. L.I. Martynenko, V.I. Spitsyn, *Selected Chapters on Inorganic Chemistry* (in Russian), MGU, Moscow (1985).
40. S.A. Kuznetsov, *Russ. J. Electrochem.*, 30 (1994) 1337-1344.
41. W. Kuhlmann, W. Sawodny, *J. Fluorine Chem.*, 9 (1997) 341-357.
42. L.A. Woodward, H.L. Roberts, *Trans. Faraday Soc.*, 52 (1956) 615-619.
43. S.S. Batsanov, *Experimental Basis of Structural Chemistry* (in Russian) Izd. Standartov, Moscow (1986).
44. H. Lux, *Z. Elektrochem.*, 45 (1939) 303-313.
45. S.A. Kuznetsov, A.L. Glagolevskaya, *Russ. J. Electrochem.*, 31 (1995) 1285-1288.
46. H.A. Oye, D.M. Gruen, *Inorg. Chem.*, 3 (1964) 836-840.
47. S.A. Kuznetsov, M. Gaune-Escard, *J. Nucl.Mater.*, 389 (2009) 108-114.
48. Yu.M. Kiselev, A. Brandt, L.I. Martynenko, V.I. Spitsyn, *Dokl. Akad. Nauk SSSR*, 246 (1979) 879-882.
49. A. Salyulev, O. Tkacheva, V. Shishkin, *Progress in Molten Salt Chemistry*, Elsevier, Amsterdam 1 (2000) 471-474.
50. D. Olander, *Nucl.Mater.*, 300 (2002) 270-272.
51. S.A. Kuznetsov, V.T. Kalinnikov, *Doklady Chemistry*, 441 (2011). 318-320.

© 2016 The Authors. Published by ESG (www.electrochemsci.org). This article is an open access article distributed under the terms and conditions of the Creative Commons Attribution license (<http://creativecommons.org/licenses/by/4.0/>).